

# From Evidence-Based Medicine to Knowledge Graph: Retrieval-Augmented Generation for Sports Rehabilitation and a Domain Benchmark

Jinning Zhang<sup>1,2†</sup>, Jie Song<sup>1,2†</sup>, Wenhui Tu<sup>‡1,2</sup>, Zecheng Li<sup>‡1,2</sup>,  
Jingxuan Li<sup>3</sup>, Jin Li<sup>4</sup>, Xuan Liu<sup>5</sup>, Taole Sha<sup>7</sup>, Zichen Wei<sup>6</sup>,  
Yan Li<sup>1,2\*</sup>

<sup>1</sup>Beijing Key Laboratory of Sports Performance and Skill Assessment,  
Beijing Sport University, Beijing, 100084, China.

<sup>2</sup>Department of Exercise Physiology, School of Sport Science, Beijing  
Sport University, Beijing, 100084, China.

<sup>3</sup>School of Sport Medicine and Physical Therapy, Beijing Sport  
University, Beijing, 100084, China.

<sup>4</sup>Rehabilitation Center, Beijing Rehabilitation Hospital, Beijing,  
100144, China.

<sup>5</sup>Optum Care Washington, Everett, Washington, 98201, USA.

<sup>6</sup>School of Management, Beijing Sport University, Beijing, 100084,  
China.

<sup>7</sup>Department of Statistics and Actuarial Science, The University of  
Hong Kong, Hong Kong, China.

\*Corresponding author(s). E-mail(s): [bsuliyan@bsu.edu.cn](mailto:bsuliyan@bsu.edu.cn);

†These authors contributed equally to this work.

## Abstract

In medicine, large language models (LLMs) commonly leverage retrieval-augmented generation (RAG) to ground outputs in up-to-date external evidence and reduce hallucinations. However, current RAG approaches focus primarily on performance improvements while overlooking evidence-based medicine (EBM) principles. This study addresses two key gaps: (1) the lack of PICO alignment between queries and retrieved evidence, and (2) the absence of evidence hierarchy considerations during reranking. We present a reusable adaptation strategy for integrating EBM into graph-based RAG, integrating the PICO framework into

knowledge graph construction and retrieval, and proposing a Bayesian-inspired reranking algorithm to calibrate ranking scores by evidence grade without introducing predefined weights. We validated this framework in sports rehabilitation, a literature-rich domain currently lacking RAG systems and benchmarks. We released a knowledge graph (357,844 nodes and 371,226 edges) and a reusable benchmark of 1,637 QA pairs. The system achieved 0.830 nugget coverage, 0.819 answer faithfulness, 0.882 semantic similarity, and 0.788 PICOT match accuracy. In a 5-point Likert evaluation, five expert clinicians rated the system 4.66–4.84 across factual accuracy, faithfulness, relevance, safety, and PICO alignment. These findings demonstrate that the proposed EBM adaptation strategy substantially improves retrieval and answer quality and is readily transferable to other clinical domains; while the released resources help address the scarcity of RAG datasets in sports rehabilitation.

**Keywords:** Large language models, Evidence-based medicine, Knowledge graph, Retrieval-augmented generation, Sports rehabilitation

## 1 Introduction

Consider the following question posed to a large language model (LLM): “My child has congenital heart disease and has just undergone surgery. How should we conduct postoperative exercise rehabilitation?” As of 2024, the evidence base for rehabilitation in children with congenital heart disease remains limited, consisting primarily of observational studies[1, 2], with authoritative guidelines only recently emerging[3]. In such cases, LLMs often provide outdated or suboptimal answers due to their training data cutoff[4].

In medicine, clinical evidence evolves rapidly. For example, the latest American College of Sports Medicine (ACSM) edition adopts the metabolic chronotropic reserve (MCR) to assess whether the heart rate response during exercise is appropriate[5], replacing the traditional 220 minus age formula, which recent studies have shown can carry significant errors[6, 7]. The ACSM has also updated exercise prescriptions for special populations (e.g., transgender individuals, older adults, and children), rehabilitation strategies for chronic diseases, and predictive equations[5]. Retrieval-Augmented Generation (RAG) is designed to incorporate such time-sensitive information, dynamically extending LLM knowledge to prevent obsolescence and reduce hallucinations[8]. In brief, RAG comprises three stages: the Retriever searches user-curated corpora in a vector database; the Augmenter filters, reranks, and injects results into the model’s context; and the Generator synthesizes retrieved information to produce answers with cited sources[8]. In medicine, the need for traceable evidence and timely information makes RAG a widely adopted approach for enhancing LLM reliability[9, 10].

With the rapid advancement of artificial intelligence (AI), RAG methods have been evolving rapidly. The seminal RAG framework by Lewis et al. employed a vector

---

<sup>‡</sup> These authors contributed equally as second authors.

retriever to recall the top- $K$  text chunks from a knowledge base, which were concatenated with the user query and fed into an LLM for answer generation[8]. In 2021, Luan et al. proposed a hybrid retrieval strategy within RAG that significantly improved the reliability of downstream tasks[11]. Specifically, this strategy fuses sparse retrieval (e.g., keyword-based methods) with dense retrieval (e.g., semantic embeddings) at the recall stage, thereby enhancing retrieval performance. Subsequently, domain-specific RAG systems for medicine began to emerge. In 2023, Shi et al. introduced MKRAG, the first to incorporate a structured medical knowledge base, and conducted systematic evaluations that established a baseline for subsequent medical RAG research[12]. The following year, RAG research began to introduce domain-specific methodological innovations for medicine. For example, the RAG<sup>2</sup> framework by Sohn et al. leverages intermediate reasoning steps generated by the LLM during answer generation to iteratively retrieve supporting evidence, thereby reducing hallucinations and enabling a traceable evidence chain[13]. Additionally, MRD-RAG by Sun et al. combines disease information trees with pseudo-medical-history indexing to develop the first multi-turn diagnostic RAG system, which substantially improves diagnostic accuracy and serves as an early prototype of Agentic RAG in medicine[14].

Returning to the original user question, the patient is a child with congenital heart disease—a special population. Recently evolved RAG frameworks typically focus on performance improvements without explicitly accounting for query-specific target populations[15–18], potentially generating population-mismatched answers (especially when limited corpus evidence leads to insufficient recall[19]). Crucially, most evaluation metrics cannot identify population mismatches. For example, semantic similarity uses cosine similarity to quantify differences between generated and reference answers at a macro level, making general phrasing far more influential than specific details; answer faithfulness measures only factual alignment between the answer and retrieved context, ignoring relevance to the query—retrieving passages about adults with congenital heart disease would not affect this metric[20]. Another key issue is that even if RAG incorporates the latest authoritative guidelines for the rehabilitation of children with congenital heart disease, these sources would still be weighted the same as earlier scattered observational evidence during retrieval[21], which violates the concept of a hierarchy of evidence[22]. The two issues above can be summarized as follows: Current medical RAG approaches neglect the evidence-based medicine (EBM) framework[23]. In particular, the Population–Intervention–Comparator–Outcome (PICO) framework and the hierarchy of evidence remain largely overlooked.

Regarding the combination of EBM and RAG, especially the integration of the PICO framework, graph-based retrieval-augmented generation (GraphRAG) shows promising potential. This paradigm leverages knowledge graphs constructed from entity-relation-attribute triples to provide a structured hierarchy for the corpus[24]. Originally, it's designed to enhance the multihop reasoning capabilities of LLMs for complex questions, which are particularly important in medical contexts[25]. However, this highly structured arrangement can also implicitly guide LLMs to retrieve from nodes aligned with the query, thereby potentially improving PICO alignment between questions and answers. Based on this, we propose the key question of this study:

- How can the EBM framework be adapted to RAG pipelines, particularly GraphRAG?

Since the pioneering work of Edge et al.[24], GraphRAG has evolved along two main trajectories: graph retrieval and graph construction[26]. The former focuses on improving retrieval efficiency and relevance, while the latter aims to enrich graph topology and enable multi-granularity retrieval. Recently, Youtu-GraphRAG, proposed by Dong et al.[26], unifies graph retrieval and graph construction through schema-bounded agentic extraction. This strategy reduces extraction noise during graph construction while enabling rapid domain adaptation through schema replacement. Essentially, it shifts the implicit retrieval constraints of traditional GraphRAG to a new paradigm of explicitly constrained retrieval by predefining the schema. In the medical domain, when we directly define the schema as PICO-related entity types, PICO mismatch between queries and retrieved chunks may be substantially reduced (Fig. 1). Accordingly, this study aims to address EBM adaptation based on the Youtu-GraphRAG framework. In particular, although the field of sports rehabilitation is resource-rich, no domain-specific RAG system or reusable benchmark currently exists. We therefore focus on this domain, curating a corpus, constructing a benchmark, and validating our framework.

In summary, the main contributions of this study are as follows:

- We curate high-quality corpora covering 21 common conditions in sports rehabilitation along with domain-relevant general guidelines, and construct a knowledge graph comprising 357,844 nodes and 371,226 relationships.
- We propose a Bayesian-inspired reranking algorithm that calibrates the ranking scores of a cross-encoder by incorporating both semantic and evidence-grade information of candidate chunks without introducing predefined weights, enabling explicit consideration of evidence hierarchy during reranking.
- We present Sports Rehabilitation RAG (SR-RAG), which integrates the EBM framework into GraphRAG pipeline through a generalizable adaptation strategy, with sports rehabilitation as the validation domain.
- We develop a reusable benchmark for sports rehabilitation comprising 1,637 QA pairs and conduct systematic evaluation of SR-RAG through automated metrics and sampled expert clinician review, both confirming system reliability.

## 2 Results

### 2.1 Knowledge Graph Construction

Following corpus preprocessing and evidence-grade annotation, we constructed a knowledge graph for sports rehabilitation based on the Youtu-GraphRAG framework. The schema for nodes, relations, and attributes was replaced with PICO-related terms to explicitly encode evidence-based query structure during graph construction(Supplementary Table S1) . The final knowledge graph consisted of 21 types of sports rehabilitation disease corpora, together with general cross-disease guidelines, comprising a total of 357,844 nodes and 371,226 edges. Of all nodes, 44,033 (12.3%) were core medical entities directly aligned with the PICO framework. Among these,

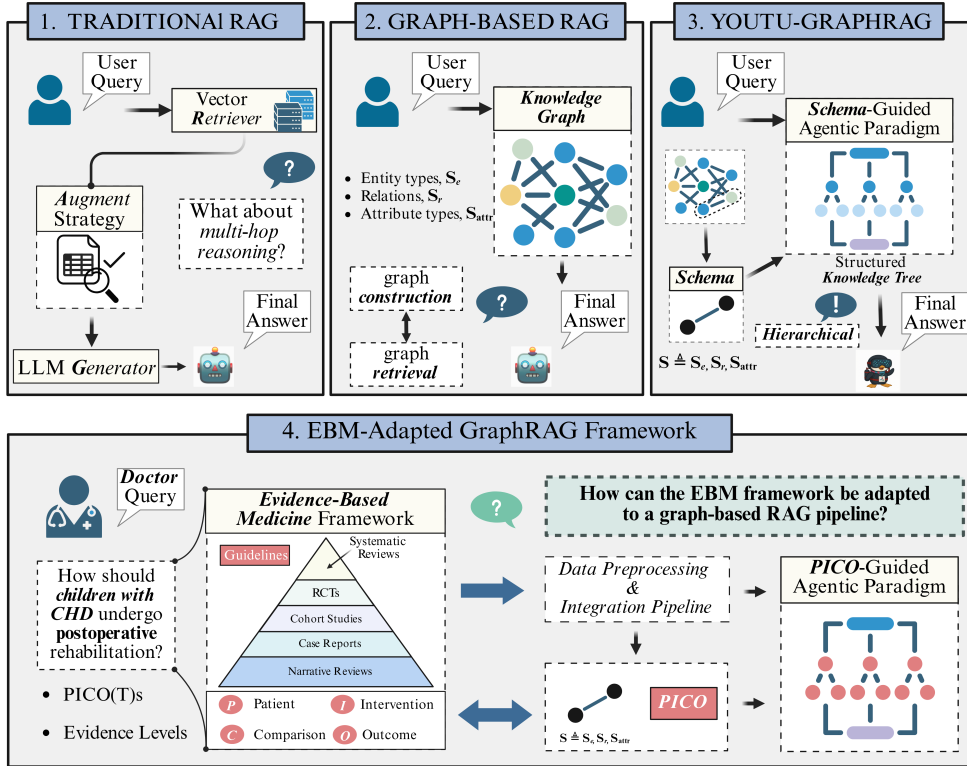


**Fig. 1** Evolution from traditional RAG to graph-based RAG and the proposed EBM-adapted GraphRAG framework integrating evidence hierarchy and the PICO framework.

Intervention nodes were most prevalent (13,866; 31.5%), followed by Condition (9,979; 22.7%), Outcome (8,609; 19.5%), and Population (6,838; 15.5%). Arm, Device, and Comparator accounted for 2,134 (4.9%), 1,569 (3.6%), and 1,038 (2.4%), respectively. The graph data are available at <https://huggingface.co/datasets/Ning311/sr-rag-knowledge-graph>.

## 2.2 Bayesian Evidence Tier Reranking

To simultaneously reflect semantic relevance and the evidence hierarchy of EBM during reranking, while avoiding the limited interpretability and transferability caused by manually predefined weights, we proposed Bayesian Evidence Tier Reranking (BETR). This algorithm utilized a Bayesian maximum a posteriori (MAP) estimation paradigm to learn bias scores among evidence grades, which were then used to calibrate the reranking scores of candidate chunks. Specifically, the calibrator constructed positive-negative pairs ( $d^+, d^-$ ) from candidate chunks and modeled the probability  $p(d^+ \succ d^- | \theta)$  that the positive example ranks above the negative in pairwise logistic form. The influence of evidence grades was captured through a set of learnable

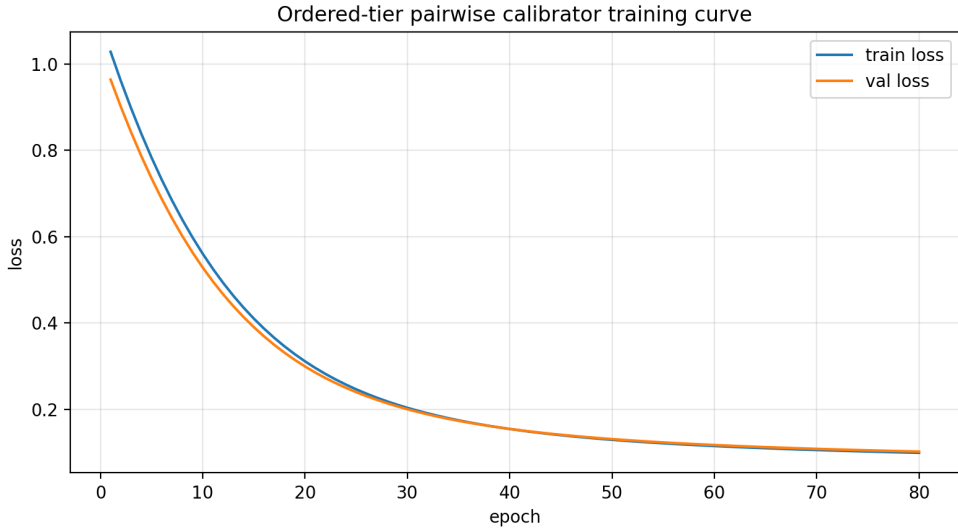


**Fig. 2** Training and validation objective curves for the ordered-grade pairwise calibrator.

grade bias scores  $u_t$ . Model parameters were learned by maximizing the log-posterior, which includes both the pairwise log-likelihood and a shrinkage prior. For detailed algorithmic steps, see the Methods section.

We partitioned the benchmark into a training set ( $n = 1310$ ) and a validation set ( $n = 327$ ), used for parameter fitting and hyperparameter selection, respectively. After fixing the candidate generation and negative sampling strategies, we constructed 26,755 pairwise samples (train=21,546; val=5,209). As shown in Fig. 2, both the training and validation objectives (negative log loss) decreased monotonically with epochs and converged at approximately 60–80 epochs. The gap between training and validation curves remained small, with no evident overfitting.

The training results were listed in Table 1. The grade biases  $u_t$  learned by BETR were strictly monotonically decreasing, consistent with EBM principles. The spacing  $\delta$  between adjacent grades was approximately constant ( $\approx 0.129$ ), indicating similar penalty magnitudes across grades under the current data distribution, with no extreme biases. Finally, the semantic score scale parameter  $a = 1.0348$  indicated minimal rescaling of the reranker score, and the final online ranking score was still mainly driven by semantic relevance, with grade bias affecting only candidates of comparable semantic similarity, which aligned with our aim. Additional training details and hyperparameters were provided in Supplementary Table S3.

### 2.3 Case Study

SR-RAG adapts Youtu-GraphRAG to accommodate medical domain tasks. Specifically, modifications focus on three key components: (1) PICO-guided Hypothetical Document Embeddings (HyDE): generates hypothetical documents with PICO soft

**Table 1** Learned grade bias parameters of BETR.

Grade	$u_t$	odds ratio	$\Delta$ from prev.
A	0.0000	1.0000	—
B	-0.1287	0.8792	0.1287
C	-0.2575	0.7729	0.1288
D	-0.3863	0.6797	0.1288
E	-0.5151	0.5974	0.1288

constraints and fuses them with dense and graph retrieval; (2) Evidence-grade-aware retrieval: leverages the grade biases  $u_t$  learned by BETR to weight candidate chunks by evidence grade, given that all literature types are manually annotated during corpus collection. Guideline evidence is retrieved separately from other evidence, forming a dual-track retrieval strategy; (3) Two-stage reranking: employs ColBERT for coarse ranking followed by a cross-encoder for fine ranking, improving robust matching of medical synonyms, abbreviations, and numeric contexts within a controlled computational budget. In this section, we selected a representative question as a case study and used actual SR-RAG logs to demonstrate the full pipeline. The LLM used was DeepSeek-V3. Fig. 3 provides an overview of the case study workflow.

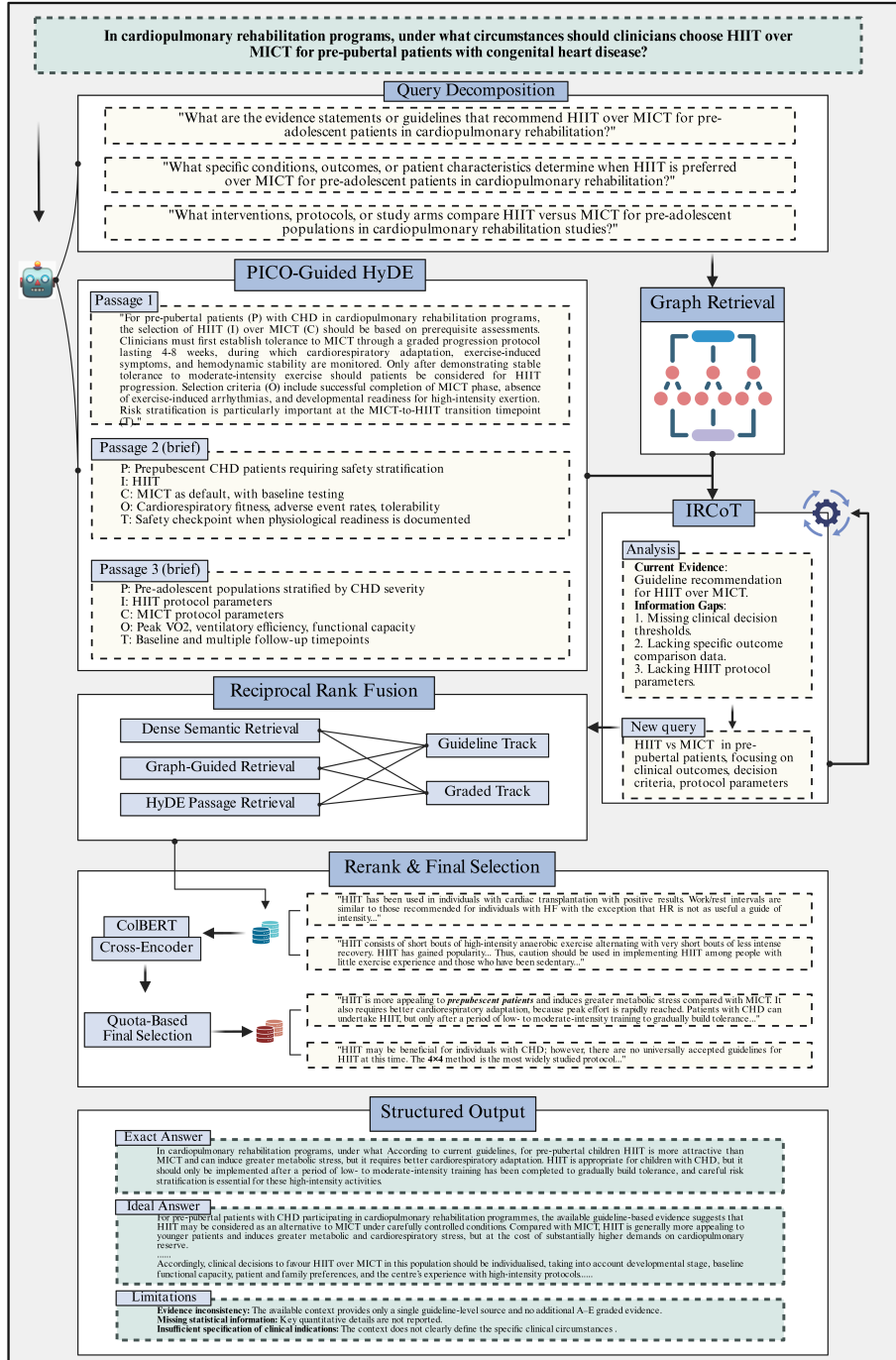


**Fig. 3** Case-study workflow of SR-RAG, illustrating PICO-guided HyDE, graph retrieval, dual-track evidence recall, reranking with BETR, and structured output.

**Query Case.** We selected the following question: “In cardiopulmonary rehabilitation programs, under what circumstances should clinicians choose high-intensity interval training (HIIT) over moderate-intensity continuous training (MICT) for prepubertal patients with congenital heart disease?” This question exhibits a clear PICO structure, requires cross-evidence integration and conditional reasoning, making it well suited as a case study.

**Query Decomposer.** This module follows the schema-enhanced decomposition paradigm of Youtu-GraphRAG: under schema constraints, complex queries are decomposed into three subproblem types—node-level retrieval, triple-level matching, and community-level verification—each aligned with the corresponding level of the hierarchical knowledge tree constructed during graph building[26]. In this case, we replaced the schema with PICO-related phrases; the resulting subproblems and retrieval paths were shown in Fig. 3.

**PICO-guided HyDE.** HyDE leverages LLMs to generate hypothetical documents relevant to a query as retrieval intermediaries, bridging the lexical gap between queries and evidence texts for retrieval augmentation[27]. In this study, we incorporated PICO soft constraints into HyDE prompts: the model preferentially reuses extractable P/I/C/O/T anchors from the query, tolerates missing fields, but is prohibited from hallucinating values for missing fields, which reduces hallucination and retrieval drift risks. In this case, the LLM generated three hypothetical documents (Fig. 3), converting the query into declarative hypothetical answers. This approach bridges the semantic gap between the query and ground truth evidence, thereby increasing their cosine similarity. Two key design principles apply: (1) many queries do not fully cover all five P/I/C/O/T dimensions, so generation should not be enforced for missing fields; (2) generating specific hypothetical values risks irrelevant value matching and should be avoided.

**EBM-Adaptive Retrieval Strategy.** SR-RAG’s adaptation to the evidence hierarchy is reflected in two mechanisms: dual-track retrieval and BETR-calibrated ranking after candidate merging. During data preprocessing, the corpus was mapped to evidence grades A–E: A = guidelines, B = systematic reviews and meta-analyses, C = randomized controlled trials (RCTs), D = cohort studies, and E = other studies (case reports, narrative reviews, observational studies). Considering that Grade A accounts for a small proportion of the overall corpus and is easily diluted by Grades B–E, we ran separate candidate generation processes on the Grade A corpus and the Grades B–E corpus with their own recall quotas at the retrieval stage, and then merged the candidate sets. BETR calibration (see Methods section) was then applied to the ranking scores for the merged candidates, ensuring that while semantic relevance remains dominant, higher grades were prioritized when the relevance is comparable.

**Three-channel Retrieval Fusion.** SR-RAG combines the ranking results from three retrieval channels using Reciprocal Rank Fusion (RRF)[28]. For any candidate window  $d$ , the RRF score is defined as:

$$\text{RRF}(d) = \sum_{c \in \{\text{Dense, Graph, HyDE}\}} \frac{1}{k + \text{rank}_c(d)}, \quad (1)$$

where  $\text{rank}_c(d)$  is the rank of window  $d$  in channel  $c$ , and  $k$  is a smoothing constant. After fusion, the pipeline follows Youtu-GraphRAG’s parallel retrieval strategy (Entity Matching, Triple Matching, Community Filtering) to generate candidate windows.

Iterative Reasoning and Reflection (IRCoT). This module follows the Agentic Retriever paradigm of Youtu-GraphRAG, enabling schema-guided iterative reasoning and reflection. In this case, IRCoT performed three iterations. An example iteration was shown in Fig. 3.

Two-Stage Cascaded Reranking Strategy. We adopted a two-stage reranking approach cascading ColBERT (mxbai-edge-colbert-v0) with a cross-encoder (BGE-reranker-v2-m3): ColBERT applies the MaxSim mechanism to coarse-rank fused candidate windows and filters to top- $K$ [29]; the cross-encoder then performs fine-grained ranking within top- $K$  to capture global semantic and logical relationships. BETR calibration was then applied to the cross-encoder logit scores to produce the final ranking score:

$$r(q, d) = \hat{a} s(q, d) + \hat{u}_{\text{Grade}(d)}, \quad (2)$$

where  $s(q, d)$  denotes the semantic score and  $\hat{u}_{\text{Grade}(d)}$  the learned grade bias (see Methods).

Quota-Based Final Selection. For final selection, we adopted a soft quota strategy: if Grade A candidates have sufficiently high scores, at least one Grade A window is retained; otherwise, selection defaults to the global top- $K$  without enforcement. Additionally, when the candidate pool is smaller than the quota target, all available items are returned to avoid padding with low-quality evidence. In this case, two key windows entered the top-2, replacing candidates with potential population mismatch risks (Fig. 3).

Structured Output. The first paragraph concisely summarizes the core answer; the second elaborates on guidelines and supporting evidence; the third compares the query and response, highlighting limitations (Fig. 3).

## 2.4 Results of automated evaluation and ablation studies

We conducted an end-to-end evaluation of SR-RAG using 1,637 benchmark queries, reporting four metrics: nugget coverage, answer faithfulness, semantic similarity, and PICOT match accuracy. We ran the same retrieval pipeline across Baichuan-M2, GPT-4o, and DeepSeek-V3, and performed ablation experiments on the best-performing model, DeepSeek-V3. All results were shown in Table 2. The benchmark is publicly available at <https://huggingface.co/datasets/Ning311/sr-rag-benchmark>.

Model performance differences. Among the three models, DeepSeek-V3 performed best overall, followed by GPT-4o (which achieved the highest answer faithfulness), with Baichuan-M2 ranking lowest. This may reflect architectural improvements in DeepSeek-V3. Although Baichuan-M2 is a medically specialized model, its relatively small parameter count (32B, compared to 671B for DeepSeek-V3) limits its capacity for the complex multi-step reasoning required by SR-RAG.

Ablation studies. We performed three ablations on DeepSeek-V3: (1) w/o HyDE: disables the PICO-guided HyDE channel, retaining only graph and dense retrieval; (2) w/o ColBERT: removes ColBERT coarse ranking, using only the cross-encoder for reranking; (3) w/o PICO-extended schema: replaces the graph construction and

retrieval schema with generic medical terms unrelated to PICO, to assess the contribution of the PICO-extended schema to query–answer alignment. The PICO-extended schema and ablation schemas are detailed in Supplementary Tables S1 and S2, respectively.

**Nugget coverage.** Nuggets denote the atomic factual units of the ground truth (GT). Because nugget coverage directly reflects answer comprehensiveness and correctness, recent RAG studies have increasingly adopted this metric[30, 31]. Specifically, we adopted the LLM-as-judge paradigm[32]: for each GT nugget, the judge returned “covered” or “not covered” based on prompt-constrained criteria, and we computed the nugget coverage per query. Results showed that DeepSeek-V3 achieved the highest score on this metric (0.830). Removing the PICO-extended schema caused a significant drop (0.830 to 0.774), indicating that structured PICO-based retrieval aids in recalling and articulating key points aligned with GT nuggets; removing HyDE or ColBERT also led to varying declines.

**Answer faithfulness.** This metric measures how faithfully the generated answer adheres to the retrieved context. GPT-4o achieved the highest score on this metric. Ablation showed that removing the PICO-extended schema slightly increased faithfulness (0.819 to 0.834), possibly because a narrower retrieval scope yields more focused context, encouraging the model to stay within well-supported evidence. However, this ablation also caused PICOT alignment to drop significantly (Table 2). Additionally, removing ColBERT had the greatest negative impact on faithfulness (0.819 to 0.752), suggesting that the absence of token-level coarse ranking significantly increased candidate noise.

**Semantic similarity.** This metric measures the cosine similarity between generated answers and GT in embedding space, primarily reflecting surface-level textual similarity. DeepSeek-V3 achieved the highest score (0.882). Notably, this metric showed a slight increase under the w/o PICO-extended schema setting (0.886), indicating that pure semantic similarity is insufficient to detect critical population or intervention mismatches in medical QA and must be complemented by domain-specific metrics such as PICOT match accuracy.

**PICOT match accuracy.** As mentioned earlier, mainstream RAG evaluation methods currently lack specific metrics for medical QA, making it difficult to detect PICO mismatches. To address this, we developed an evaluation paradigm analogous to nugget coverage. During benchmark construction, we extracted PICOT fields from GT as gold standards and extracted corresponding fields from system outputs for item-by-item matching (synonymous expressions were permitted; missing GT fields were excluded). We then computed the overall field match rate. This metric directly quantifies critical mismatches between query and answer, such as population or intervention discrepancies. Results showed that DeepSeek-V3 achieved the best performance on this metric (0.788). In ablation, replacing the PICO-extended schema with generic medical entity types significantly lowered match accuracy (0.788 to 0.701), demonstrating the effectiveness of PICO as a schema within the GraphRAG paradigm. Disabling HyDE also led to a drop (0.788 to 0.723), confirming that PICO-guided HyDE is critical for PICO matching.

**Table 2** Automated evaluation and ablation results on the SR-RAG benchmark.

Model	Pipeline	Nugget coverage	Faithfulness	Semantic similarity	PICO match
GPT-4o[33]	SR-RAG	0.825	0.842	0.862	0.762
Baichuan-M2[34]	SR-RAG	0.740	0.785	0.806	0.755
DeepSeek-V3[35]	SR-RAG	0.830	0.819	0.882	0.788
DeepSeek-V3	w/o Hyde	0.819	0.801	0.879	0.723
DeepSeek-V3	w/o ColBERT	0.798	0.752	0.884	0.740
DeepSeek-V3	w/o PICO-extended schema	0.774	0.834	0.886	0.701

## 2.5 Results of doctor evaluation

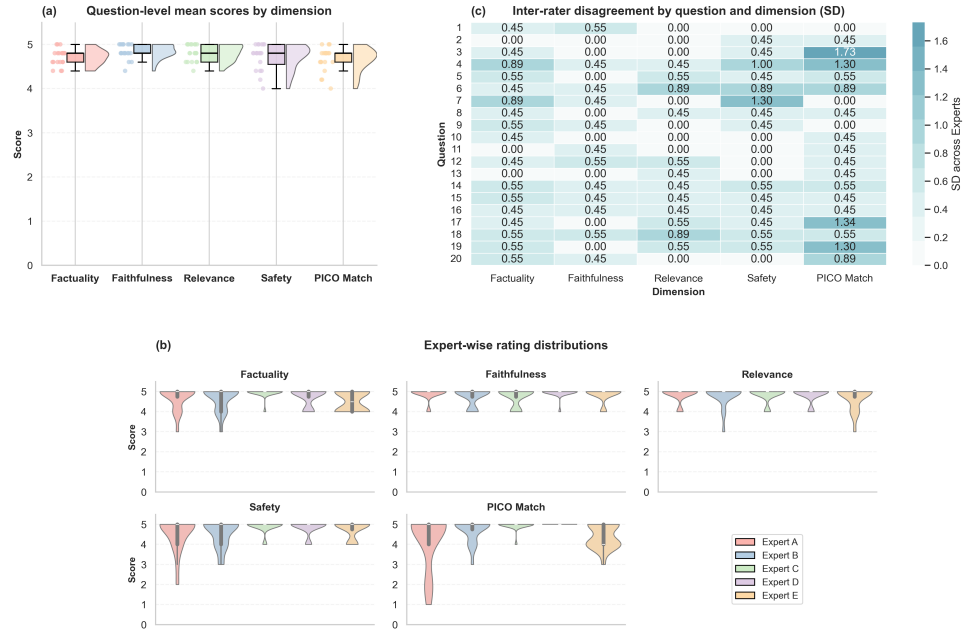


**Fig. 4** Expert clinician evaluation results, including rating distributions and inter-rater disagreement across dimensions.

We randomly sampled 20 questions and invited five sports rehabilitation experts to conduct manual evaluation. Each expert reviewed the same set of questions and materials, with each review taking approximately one hour. Assessment used a 1–5 Likert scale with independent scoring across five dimensions: medical factual accuracy (factuality), answer faithfulness (faithfulness), answer relevance (relevance), safety, and PICOT alignment (PICO match) (Fig. 4). For detailed evaluation procedures and scoring criteria, see the Methods section.

SR-RAG received high scores across all five dimensions, with most ratings in the 4–5 range (Fig. 4(a)). Aggregated mean ( $\pm$  SD) scores were: medical factual accuracy  $4.71 \pm 0.50$ , answer faithfulness  $4.84 \pm 0.37$ , answer relevance  $4.81 \pm 0.44$ , safety  $4.72 \pm 0.57$ , and PICOT alignment  $4.66 \pm 0.76$ . Notably, answer faithfulness and answer relevance had the highest means with the lowest variability, indicating that the system generated responses closely aligned with queries. PICOT alignment had the largest SD (0.76), suggesting greater susceptibility to variation in question format.

Fig. 4(b–c) presents inter-rater consistency analysis. Mean inter-rater SD for the five dimensions was: medical factual accuracy 0.46, answer faithfulness 0.28, answer relevance 0.33, safety 0.42, and PICOT alignment 0.63. Reviewer disagreement was greatest for PICOT alignment, driven primarily by a few outlier questions (e.g., Q3: SD = 1.73; Q17: SD = 1.34), as shown in Fig. 4(c). Overall, manual evaluation aligned with automated assessment results, demonstrating SR-RAG’s reliability in sports rehabilitation clinical QA.

### 3 Discussion

In this study, we present SR-RAG, an EBM-adapted GraphRAG framework for sports rehabilitation. SR-RAG builds on Youtu-GraphRAG and adapts it to medical tasks through PICO-guided HyDE, dual-track evidence retrieval, and BETR-calibrated two-stage reranking. SR-RAG focuses on sports rehabilitation. We adopted Youtu-GraphRAG’s community compression algorithm to construct the first knowledge graph for sports rehabilitation and generate 1,637 reusable QA pairs for evaluation. SR-RAG’s reliability was validated through both automated evaluation and expert review.

During graph construction, we did not perform ontology normalization; consequently, the same clinical concept expressed differently across studies appears as multiple nodes, yielding a long-tailed distribution with many nodes and edges. We retained the original graph structure for three reasons. First, standard ontologies in sports rehabilitation are diverse with rich terminological variation, making automatic normalization challenging and risking erroneous merging of studies that are semantically similar yet differ in disease subtype, intervention parameters, or follow-up duration[36]. Second, Youtu-GraphRAG already clusters and consolidates graph structure via dual-perception community compression; additional concept merging may introduce noise. Third, downstream RAG tasks already handle synonymous expressions implicitly via two-stage reranking with satisfactory retrieval and QA performance, so normalization offers limited additional benefit. Accordingly, we retained the original graph structure and plan to explore finer-grained ontology alignment in future work.

We address the core question of this paper: how to adapt the EBM framework to RAG systems, via generalizable components that can be reused across clinical domains.

- **Evidence hierarchy principles.**

- At the data collection stage, we distinguish literature types and manually label each corpus entry with its evidence grade. This practice is readily transferable

to future medical RAG systems. Given the cost of manual labeling, a reasonable fallback is to use LLMs to read abstracts and assign document types automatically.

- At the reranking stage, we propose BETR, a Bayesian-inspired algorithm that minimizes manual intervention while improving weight interpretability. Because BETR only requires reranker logits and ordered evidence grades, the same formulation can be reused across medical domains without redesigning ad-hoc weighting rules.
  - SR-RAG stratifies recall by evidence grade: Grade A and Grades B–E evidence are recalled separately to ensure guideline coverage. The two candidate sets are then merged, BETR calibrates the ranking scores, and a soft quota strategy avoids forcing semantically irrelevant evidence into the final selection. This dual-track retrieval strategy is domain-agnostic and can be applied to any corpus with tiered evidence sources. This mirrors clinical retrieval practice: guidelines and consensus are prioritized, with research evidence supplementing details and applicability boundaries.
- **PICO principles.** Beyond replacing the schema with PICO-related terms, we enhance the HyDE method. Traditional HyDE narrows the semantic gap between queries and corpus by generating hypothetical documents via LLMs, thereby boosting similarity with relevant passages[27]. Building on this, we modify prompts to add soft PICOT constraints for medical adaptation, with effectiveness demonstrated experimentally.

Notably, recent RAG studies in medicine have begun to emphasize integration with EBM. PICOs-RAG, proposed by Sun et al.[37], improves PICO alignment in QA by expanding and standardizing user questions and extracting PICO elements for retrieval. While this approach is similar to ours, the key distinction is the rewriting target—they reformulate the query, whereas HyDE generates hypothetical answers. Rewriting the question enables explicit PICO standardization and effective matching via sparse keyword retrieval. However, a semantic gap typically exists between user queries and retrieved documents[38]. Queries are often short or vague, creating an asymmetric match against concrete, comprehensive documents and weakening retrieval effectiveness. Hypothetical documents can bridge this semantic gap and improve retrieval matches, but also pose a risk of hallucination[39]. In this study, we extracted PICOT elements via prompts without forcing completion, avoiding fabrication of missing fields or specific values to mitigate hallucination risk.

Similar to PICOs-RAG, Quicker emphasizes the PICO principle and incorporates it throughout the pipeline[40]. In question decomposition, the LLM structures clinical problems into PICO elements. In document retrieval, PICO components are expanded into search terms and combined into Boolean queries. In study screening, PICO elements serve as inclusion and exclusion criteria to guide full-text assessment. Quicker also implements the GRADE system for EBM principles[22], systematically evaluating evidence quality across five dimensions: risk of bias, inconsistency, indirectness, imprecision, and publication bias. This multidimensional paradigm goes beyond SR-RAG’s current approach, which relies on document type as the primary dimension. However,

Quicker and BETR are methodologically complementary: GRADE provides quantitative within-study evidence quality assessment, whereas evidence hierarchy focuses on cross-study comparison.

Some RAG systems have begun to focus on the issue of evidence hierarchy. Med-R<sup>2</sup> decomposes the EBM workflow into stages: clinical question construction, evidence retrieval and evaluation, and evidence application[41]. In the evidence evaluation stage, it introduces a dedicated evidence reranking module. This module maps evidence hierarchy to confidence levels, which are then incorporated as factors in the reranking score. However, this approach is based on a manually defined linear mapping  $f_h(x) = 9 - e + 1$  that converts hierarchy into scores, which presents the following problems: (1) Excessive manual intervention: the nine-level division and equal-interval assumption lack justification; (2) Poor interpretability of coupled multiplication after mapping: once the hierarchical score is multiplied by document type and usefulness scores, it becomes difficult to disentangle the independent contribution of each factor; (3) Lack of cross-system reusability: fixed rules cannot adapt to the evidence distribution in different domains. For example, RCTs are scarce for certain rare diseases, and rule-based weighting cannot simultaneously accommodate semantic relevance. META-RAG further refines the evidence screening framework by drawing on meta-analysis principles to rerank evidence across three dimensions: reliability, heterogeneity, and extrapolation[21]. Notably, its heterogeneity analysis introduces the DerSimonian-Laird random-effects model to explicitly exclude evidence inconsistent with the mainstream conclusion, and its extrapolation analysis employs PIO matching to assess evidence applicability to the current patient, providing a more systematic framework than the single linear mapping of Med-R<sup>2</sup>. However, the final ranking score in META-RAG still relies on a manually defined formula  $S_j = r_j^2 \cdot T_j$ , where the weight formulation lacks theoretical justification and the fixed rules cannot adapt to evidence distributions in different domains. The BETR algorithm proposed in this study addresses these limitations by learning grade bias parameters through Bayesian maximum a posteriori estimation, avoiding manual weight specification while ensuring cross-domain transferability.

Regarding the guideline-priority principle, GARMLE-G by Li et al. uses only clinical practice guidelines as the external knowledge source[42]. Unlike traditional RAG, it returns original guideline segments as answers rather than allowing free-form generation. This is conceptually aligned with SR-RAG’s dual-track retrieval strategy; both prioritize authoritative clinical guidance over primary research.

Finally, most public datasets in sports rehabilitation consist of multimodal data for motion analysis or injury prediction, oriented toward biomechanics or computer vision[43–45], with very limited resources for LLM research. This study leveraged curated corpora to create 1,637 QA pairs for evaluation through automated generation pipelines combined with manual review. Additionally, we constructed a full-scale knowledge graph dataset from the entire corpus using Youtu-GraphRAG’s graph construction pipeline. This partially addressed the current scarcity of LLM-related datasets in sports rehabilitation. However, we did not include rare diseases or conditions lacking authoritative guidelines. Future work could supplement benchmarks for additional conditions to enrich domain coverage.

Our study has the following limitations. First, the scale of expert-reviewed questions is limited, potentially introducing evaluation bias. We mitigate this by (1) inviting multiple experts with standardized one-hour review sessions and (2) implementing fully automated evaluation across the entire dataset. Second, the absence of ontology normalization in the knowledge graph introduces noise and structural redundancy. Finally, our system focuses on macro-level comparisons across study types without assessing within-study evidence quality. In contrast, Quicker implements the GRADE system to evaluate five quality dimensions at the individual study level[40], and META-RAG introduces heterogeneity analysis to filter inconsistent findings and extrapolation analysis to assess patient-specific applicability[21]. Integrating such fine-grained quality assessment into BETR-calibrated reranking represents a promising direction. More broadly, future work should pursue tighter integration of EBM principles throughout the RAG pipeline.

## 4 Methods

### 4.1 Corpus Collection and Data Preprocessing

Corpus collection was performed by four graduate students from the Department of Sports Science. We first defined inclusion criteria based on common conditions in clinical sports rehabilitation, excluding conditions with scarce literature or lacking authoritative guideline support. Next, we retrieved open-access and institution-subscribed literature on each disease from major databases, such as PubMed and Embase, and supplemented materials from authoritative sports rehabilitation organization websites. Referring to established evidence grading frameworks[46–48], we categorized the literature types as follows: guidelines and expert consensus, systematic reviews and meta-analyses, RCTs, cohort studies, and other research (case reports, narrative reviews, observational studies, and other corpus). Through targeted search strategies and manual abstract review, we ensured accurate evidence-grade assignment for each document. Ultimately, we compiled a domain corpus covering 21 conditions, mapped to evidence grades A–E.

During data preprocessing, we used Docling to convert PDFs to Markdown and extract hierarchical structure (titles, sections, tables)[49]. We then applied regular expressions to remove header and footer noise (e.g., copyright statements, references) and standardized numeral and unit formatting to reduce cross-document inconsistencies. Finally, we recorded each document’s evidence grade in metadata for subsequent evidence-grade-aware retrieval and BETR calibration.

In the chunking phase, we adopted an LLM-aware hybrid chunking strategy. First, MarkdownHeaderTextSplitter divided documents into sections by heading level[50]. Each section was further split into numbered atomic blocks preserving paragraph structure. Under prompt constraints, the LLM performed semantic grouping of atomic blocks and returned group IDs. The program concatenated each group into final evidence windows. This strategy aimed to enhance the semantic integrity and clinical information density of the windows while preserving paragraph boundaries, aligning with recent LLM-aware chunking methods such as AutoChunker, MetaChunking, and LumberChunker[51–53].

---

**Algorithm 1** Bayesian Evidence Tier Reranking

---

**Require:** Disjoint query splits  $\mathcal{Q}_{\text{train}}, \mathcal{Q}_{\text{val}}$  with gold windows  $\mathcal{W}^*(q)$ ; candidate generator  $\text{Cand}(\cdot)$ ; reranker  $f_\theta$  returning logit  $s(q, d)$ ; ordered evidence grades  $A \succ B \succ C \succ D \succ E$ ; grade function  $\text{Grade}(d) \in \{A, B, C, D, E\}$ ; negatives per positive  $K$ ; shrinkage scale  $\tau$  (selected via grid search on  $\mathcal{Q}_{\text{val}}$  and fixed for all experiments); scale prior  $\sigma_a$  for  $a$ .

**Ensure:** Calibrator parameters  $(\alpha, \delta_B, \delta_C, \delta_D, \delta_E)$  and online ranking score  $r(q, d)$ .

**Step 1: Build pairwise records (train split)**

- 1:  $\{\mathcal{P}_q\}_{q \in \mathcal{Q}_{\text{train}}} \leftarrow \emptyset$
- 2: **for**  $q \in \mathcal{Q}_{\text{train}}$  **do**
- 3:    $\mathcal{C}_q \leftarrow \text{Cand}(q); \mathcal{C}_q^+ \leftarrow \mathcal{C}_q \cap \mathcal{W}^*(q); \mathcal{C}_q^- \leftarrow \mathcal{C}_q \setminus \mathcal{W}^*(q)$
- 4:   If  $\mathcal{C}_q^+ = \emptyset$  or  $\mathcal{C}_q^- = \emptyset$ , set  $\mathcal{P}_q \leftarrow \emptyset$ .
- 5:   Else form  $\mathcal{P}_q \subseteq \mathcal{C}_q^+ \times \mathcal{C}_q^-$  by sampling  $K$  negatives per  $d^+ \in \mathcal{C}_q^+$ .
- 6:   For each  $(d^+, d^-) \in \mathcal{P}_q$ , compute  $\Delta s = s(q, d^+) - s(q, d^-)$  and  $t^\pm = \text{Grade}(d^\pm)$ .
- 7: **end for**

**Step 2: Ordered grade effects and MAP fit**

Define  $u_A = 0$ ,  $u_B = -\delta_B$ ,  $u_C = -(\delta_B + \delta_C)$ ,  $u_D = -(\delta_B + \delta_C + \delta_D)$ ,  $u_E = -(\delta_B + \delta_C + \delta_D + \delta_E)$ , with  $\delta_B, \delta_C, \delta_D, \delta_E \geq 0$ .

Reparameterize  $a = \exp(\alpha)$ .

Fit  $(\alpha, \delta_B, \delta_C, \delta_D, \delta_E)$  by maximizing the query-normalized MAP objective:

$$\max_{\alpha, \delta_B, \delta_C, \delta_D, \delta_E \geq 0} \frac{1}{|\mathcal{Q}_{\text{train}}|} \sum_{q \in \mathcal{Q}_{\text{train}}} \frac{1}{\max(1, |\mathcal{P}_q|)} \sum_{(d^+, d^-) \in \mathcal{P}_q} \log \sigma(a \Delta s + u_{t^+} - u_{t^-}) - \frac{1}{2\tau^2} (\delta_B^2 + \delta_C^2 + \delta_D^2 + \delta_E^2) - \frac{1}{2\sigma_a^2} \alpha^2.$$

where  $\sigma(z) = (1 + e^{-z})^{-1}$ .

**Step 3: Online ranking**

- 8: For a new query  $q$  and each candidate window  $d \in \text{Cand}(q)$ , set  $a = \exp(\alpha)$  and  $t = \text{Grade}(d)$ .
  - 9: Compute  $r(q, d) = a s(q, d) + u_t$  and rank by  $r(q, d)$ .
- 

## 4.2 BETR Algorithm Workflow

The evidence hierarchy principle in EBM was integrated into the reranking pipeline to optimize ranking order. In existing literature, evidence-hierarchy-based reranking paradigms mostly rely on subjective preset scores, yielding heuristic weighting schemes[41]. Such schemes introduce excessive manually defined rules that reduce interpretability and preclude cross-system reuse. To address this, we proposed BETR. This algorithm introduced evidence hierarchy as an ordered structure into the ranking calibrator, leveraging a data-driven paradigm to improve weight interpretability and cross-system reusability. The complete workflow is presented in Algorithm 1.

**Task Definition and Objective.** Given a clinical question  $q$  and a candidate evidence window  $d$ , the reranker outputs an uncalibrated relevance score  $s(q, d)$ . For the candidate set  $\mathcal{C}_q$ , we aimed to combine the relevance score  $s(q, d)$  with evidence hierarchy  $\text{Grade}(d) \in \{A \succ B \succ C \succ D \succ E\}$  to yield a unified ranking score  $r(q, d)$  satisfying: (1) when semantic relevance differences are large,  $s(q, d)$  dominates the ranking; (2) when candidates have comparable  $s(q, d)$ , higher evidence grades receive higher final scores. This study adopted a unified five-grade evidence hierarchy: A = guidelines and expert consensus, B = systematic reviews and meta-analyses, C = RCTs, D = cohort studies, E = other research (case reports, narrative reviews, observational studies, and other corpus).

**Training Labels.** For each question  $q$ , candidate windows included in the reference evidence chain serve as positive examples:  $\mathcal{C}_q^+ = \mathcal{C}_q \cap \mathcal{W}^*(q)$ ; the remainder serve as negatives:  $\mathcal{C}_q^- = \mathcal{C}_q \setminus \mathcal{W}^*(q)$ . This design avoids per-item manual annotation and aligns the ranking objective with evidence window selection.

**Pairwise Ranking Objective.** BETR adopts a pairwise learning-to-rank approach[54], learning preferences through pairwise comparisons. Specifically, for the candidate pool of question  $q$ , we construct positive-negative pairs  $(d^+, d^-)$  with  $d^+ \in \mathcal{C}_q \cap \mathcal{W}^*(q)$  and  $d^- \in \mathcal{C}_q \setminus \mathcal{W}^*(q)$ , and model preference probability via the Bradley-Terry model[55]:

$$P(d^+ \succ d^- \mid q) = \sigma(a\Delta s + u_{t+} - u_{t-}), \quad (3)$$

where  $\Delta s = s(q, d^+) - s(q, d^-)$  is the semantic relevance difference;  $t^+ = \text{Grade}(d^+)$  and  $t^- = \text{Grade}(d^-)$  denote evidence grades;  $u_t$  is the grade bias;  $a > 0$  is the scale parameter; and  $\sigma(\cdot)$  is the sigmoid function. This formulation jointly considers two signals: (1) semantic relevance difference  $\Delta s$ , and (2) evidence grade difference  $u_{t+} - u_{t-}$ . When semantic scores are comparable, windows with higher evidence grades receive additional positive bias.

**Ordered hierarchical parameterization.** To explicitly encode a pyramid-shaped evidence hierarchy and prevent grade inversion under noisy labels, we fix the grade ordering as  $A \succ B \succ C \succ D \succ E$  and adopt monotonically constrained incremental parameterization for grade effects:

$$\begin{aligned} u_A &= 0, \\ u_B &= -\delta_B, \\ u_C &= -(\delta_B + \delta_C), \\ u_D &= -(\delta_B + \delta_C + \delta_D), \\ u_E &= -(\delta_B + \delta_C + \delta_D + \delta_E). \end{aligned} \quad (4)$$

where  $\delta_B, \delta_C, \delta_D, \delta_E \geq 0$ . This form naturally guarantees  $u_A \geq u_B \geq u_C \geq u_D \geq u_E$ , yielding an evidence-grade pyramid consistent with EBM.

We then cast BETR parameter estimation in a Bayesian framework, jointly learning the scale parameter  $a$  and grade increments  $\delta = (\delta_B, \delta_C, \delta_D, \delta_E)$  via MAP estimation.

Prior distribution. We impose zero-centered priors on the parameters, encoding the default assumption of no grade bias.

$$\alpha \sim \mathcal{N}(0, \sigma_a^2), \quad \delta_i \sim \mathcal{N}^+(0, \tau^2), \quad i \in \{B, C, D, E\} \quad (5)$$

where  $\mathcal{N}^+$  denotes a Gaussian truncated to nonnegative values, ensuring grade monotonicity. This prior has maximum density at  $\delta = 0$ , implying that ranking defaults to being driven by semantic relevance  $s(q, d)$ . Meanwhile, the prior for  $\alpha$  is centered at 0, corresponding to the default  $a = \exp(\alpha) \approx 1$ , meaning that semantic scores and grade biases are summed on the same scale. This prior assumption aligns with standard reranking, which orders results solely by relevance scores.

Likelihood function. Given parameters  $(\alpha, \delta)$ , the likelihood of the observed pairwise preference data  $(d^+ \succ d^-)$  is

$$P(\mathcal{D} | \alpha, \delta) = \prod_{q \in \mathcal{Q}_{\text{train}}} \prod_{(d^+, d^-) \in \mathcal{P}_q} \sigma(a \Delta s + u_{t^+} - u_{t^-}), \quad (6)$$

where  $a = \exp(\alpha)$  and  $\Delta s = s(q, d^+) - s(q, d^-)$ .

Posterior and MAP estimations. According to Bayes' theorem[56], the posterior distribution is proportional to the product of the likelihood and priors:

$$P(\alpha, \delta | \mathcal{D}) \propto P(\mathcal{D} | \alpha, \delta) \cdot P(\alpha) \cdot P(\delta). \quad (7)$$

Taking the logarithm and normalizing, the MAP objective is equivalent to

$$\begin{aligned} \max_{\alpha, \delta_B, \delta_C, \delta_D, \delta_E \geq 0} \quad & \frac{1}{|\mathcal{Q}_{\text{train}}|} \sum_{q \in \mathcal{Q}_{\text{train}}} \frac{1}{\max(1, |\mathcal{P}_q|)} \sum_{(d^+, d^-) \in \mathcal{P}_q} \log \sigma(a \Delta s + u_{t^+} - u_{t^-}) \\ & - \frac{1}{2\tau^2} (\delta_B^2 + \delta_C^2 + \delta_D^2 + \delta_E^2) - \frac{1}{2\sigma_a^2} \alpha^2. \end{aligned} \quad (8)$$

The first term is the query-normalized pairwise log-likelihood, where we average within each query to avoid overweighting queries with more sampled pairs. The remaining terms are quadratic shrinkage penalties corresponding to the Gaussian priors on  $\alpha$  and  $\delta$ , respectively.

This framework offers several advantages: (1) the prior provides interpretable default behavior, treating grade biases as minimum necessary adjustments; (2) the posterior is likelihood-dominated when data are ample and shrinks toward the prior when data are scarce, achieving adaptive regularization; (3) the hyperparameter  $\tau$  is selected via grid search on a validation set and fixed across all experiments, offering high interpretability: it quantifies prior confidence in the assumed grade effects, thereby minimizing manual intervention.

Training details. We split benchmark queries into non-overlapping sets:  $\mathcal{Q}_{\text{train}}$  for fitting calibrator parameters, and  $\mathcal{Q}_{\text{val}}$  for hyperparameter selection and early stopping via grid search. Splitting was query-grouped, ensuring that candidate windows for the same query did not span sets, thereby preventing information leakage. During BETR

training, candidate sets  $\mathcal{C}_q$  were constructed using the same candidate generation process  $\text{Cand}(\cdot)$  as at inference, reducing distribution shift.

Final reranking score. At inference time, for any candidate window  $d \in \mathcal{C}_q$ , the final BETR ranking score is

$$r(q, d) = \hat{a} s(q, d) + \hat{u}_{\text{Grade}(d)}. \quad (9)$$

That is, the scale-calibrated semantic relevance score is combined with the corresponding evidence-grade bias.

### 4.3 PICO-extended Schema and Knowledge Graph Construction

During knowledge graph construction, we instantiated the Youtu-GraphRAG seed schema as a PICO-extended schema and followed its graph construction workflow to build the knowledge graph over the full corpus.

Schema Definition and Constrained Extraction. Following Youtu-GraphRAG, the schema is defined as

$$\mathcal{S} \triangleq \langle \mathcal{S}_e, \mathcal{S}_r, \mathcal{S}_{\text{attr}} \rangle, \quad (10)$$

where  $\mathcal{S}_e$ ,  $\mathcal{S}_r$ , and  $\mathcal{S}_{\text{attr}}$  represent the sets of entity, relation, and attribute types, respectively. Based on this schema, the LLM extraction agent performs constrained triple extraction for each document (denoted by  $x$ ):

$$\mathcal{T}(x) = \left\{ (h, r, t), (e, r_{\text{attr}}, e_{\text{attr}}) \mid \{f(h), f(t), f(e)\} \in \mathcal{S}_e, \{r, r_{\text{attr}}\} \in \mathcal{S}_r, e_{\text{attr}} \in \mathcal{S}_{\text{attr}} \right\}. \quad (11)$$

Here,  $(h, r, t)$  denotes an entity-relation-entity triple, and  $(e, r_{\text{attr}}, e_{\text{attr}})$  an entity-attribute pair;  $f(\cdot)$  maps text spans to types, constraining the extraction space and suppressing noise.

Instantiation of the PICO-extended schema. To explicitly incorporate the PICO framework into extraction constraints, we instantiate  $\mathcal{S}$  as a collection of PICO-related types: (1) entity types  $\mathcal{S}_e^{\text{PICO}}$ : `Population`, `Condition`, `Intervention`, `Comparator`, `Outcome`, `Timepoint`, plus domain-specific extensions frequently occurring in sports rehabilitation literature (e.g., `Arm`, `Device`); (2) relation types  $\mathcal{S}_r^{\text{PICO}}$ : directed relations linking studies to PICO entities (e.g., `has_population`, `has_condition`, `uses_intervention`, `compares_to`, `reports_outcome`); (3) attribute types  $\mathcal{S}_{\text{attr}}^{\text{PICO}}$ : key dimensions refining PICO elements (e.g., `age_bin`, `followup_weeks`, `measure_name`, `protocol_params`). A complete list is provided in Supplementary Table S1.

Schema self-expansion. Youtu-GraphRAG allows agents to propose schema extensions based on document content:

$$\Delta\mathcal{S} = \langle \Delta\mathcal{S}_e, \Delta\mathcal{S}_r, \Delta\mathcal{S}_{\text{attr}} \rangle = \mathbb{I}[f_{\text{LLM}}(x, \mathcal{S}) \odot \mathcal{S}] \geq \mu, \quad (12)$$

where  $\mu$  is the confidence threshold for accepting new schema elements, and  $\Delta\mathcal{S}$  contains candidate extensions for entities, relations, and attributes, respectively. For our task, this mechanism enables graph and index updates across disease subtypes.

Dually-perceived community compression and knowledge tree indexing. To reduce density and noise in the raw triple graph and shorten retrieval context, we adopted Youtu-GraphRAG’s dually-perceived community detection. The affinity between node  $e_i$  and community  $\mathcal{C}_m$  is defined as

$$\phi(e_i, \mathcal{C}_m) = \underbrace{\mathbb{S}_r(e_i, \mathcal{C}_m)}_{\text{relational}} \oplus \lambda \underbrace{\mathbb{S}_s(e_i, \mathcal{C}_m)}_{\text{semantic}}, \quad (13)$$

where  $\mathbb{S}_r$  measures Jaccard similarity over relation-type sets  $\Psi(\cdot)$ ,  $\mathbb{S}_s$  measures subgraph semantic similarity, and  $\lambda$  is a trade-off coefficient. Iteratively, the algorithm performs pairwise community merging based on the following threshold criterion:

$$\mathbb{E}[\phi(e_i, \mathcal{C}_a^{(t)})] - \mathbb{E}[\phi(e_i, \mathcal{C}_b^{(t)})] < \epsilon. \quad (14)$$

Ultimately, the community structure forms a four-layer knowledge tree  $\mathcal{K} = \bigcup_{\ell=1}^4 L_\ell$ :  $L_4$  = community,  $L_3$  = keyword,  $L_2$  = entity-relation triple,  $L_1$  = attribute. This knowledge tree serves as a structured index for subsequent graph retrieval and community filtering.

#### 4.4 SR-RAG Pipeline

As previously mentioned, SR-RAG introduced three key improvements to Youtu-GraphRAG: (1) a PICO-guided HyDE channel fused with graph retrieval via RRF; (2) two-stage reranking using ColBERT and a cross-encoder; (3) evidence-grade-aware retrieval that recalls guideline evidence separately to prevent dilution, followed by BETR-based reranking and a soft quota strategy to exclude semantically irrelevant candidates. For specific hyperparameter settings, see Supplementary Table S3.

PICO-guided HyDE retrieval channel. The original HyDE method addresses poor zero-shot dense retrieval performance without relevance annotations[27]. LLMs generate several hypothetical documents related to a user query, which are subsequently used for dense retrieval in the corpus. This paradigm tolerates factual errors in hypothetical documents: because retrieval relies on dense embeddings rather than lexical matching, semantic similarity is preserved even when generated content contains inaccuracies[27]. Subsequent work identified another advantage of HyDE: bridging the semantic gap between queries and documents[38]. In RAG, document-form inputs generally outperform raw question-form queries; thus, HyDE effectively improves retrieval quality and downstream performance. Based on this finding, we incorporated PICO soft constraints into the HyDE prompt: available P/I/C/O/T keywords were extracted from the query as anchors (missing fields are permitted). Hypothetical documents must reuse these anchors and are prohibited from fabricating missing fields. This design ensures HyDE serves purely as a retrieval intermediary for semantic alignment, without deviating from the original query’s PICO elements. The specific prompts are detailed in Supplementary Listing S1.

Two-stage reranking. We first used ColBERT as the coarse ranking model. Specifically, we used mxbai-edge-colbert-v0, which was recently proposed by Clavié et al.[57]. ColBERT uses the MaxSim mechanism for scoring:

$$s_{\text{col}}(q, d) = \sum_{i=1}^{|q|} \max_{j \leq |d|} \cos(\mathbf{e}_i^q, \mathbf{e}_j^d) \quad (15)$$

Here,  $\mathbf{e}_i^q$  and  $\mathbf{e}_j^d$  denote the  $i$ -th and  $j$ -th token embeddings of the query and window, respectively. The MaxSim mechanism computes, for each query token, its maximum similarity with any window token and sums across tokens[29], improving sensitivity to medical abbreviations, scale names, and synonyms while increasing matching robustness[58].

After coarse ranking, we used BGE-reranker-v2-m3 as a cross-encoder to perform fine-grained ranking on the top- $K$  high-scoring candidates[59]. The cross-encoder jointly encodes the query and each candidate window via concatenation, enabling full interaction through multiple self-attention layers and outputting an overall relevance logit  $s(q, d)$ . The computational cost of the cross-encoder increases linearly with the number of candidates. By adopting a two-stage pipeline, the system reduces reranking time and computational cost while balancing precise term matching and semantic understanding of long texts.

Evidence-grade-aware retrieval and scoring. To ensure retrieval and ranking align with EBM principles, we explicitly introduced evidence-grade information at both the candidate generation and scoring stages. First, the corpus was partitioned by annotated evidence grade into Grade A and Grades B–E, forming two candidate pools. Candidate generation and truncation were performed separately on each pool. The candidate sets were then merged, and initial reranking yielded cross-encoder logit scores. BETR calibration was then applied for final global ranking:

$$r(q, d) = \hat{a} s(q, d) + \hat{u}_{\text{Grade}(d)}. \quad (16)$$

This design enables the system to prioritize higher-grade evidence when candidate relevance is comparable.

#### 4.5 Benchmark Construction

To facilitate automated evaluation of SR-RAG, we created 1,637 QA pairs using a combination of LLM generation and human review. The benchmark composition by sub-condition and guideline set is summarized in Supplementary Table S4. Given the unique logic of SR-RAG’s QA process and to ensure both reliable evaluation and cross-system reusability, we adopted the following pipeline.

First, using the corpus with completed evidence-grade annotation and chunking, we performed stratified sampling by evidence grade to obtain candidate evidence windows, filtering those with insufficient information density or lacking substantive clinical conclusions. For each candidate window, an LLM generated a clinical question strictly corresponding to the window’s core conclusion while simultaneously extracting PICOT elements. During generation, questions had to be directly supported by the window; inclusion of information not present in the window was prohibited[60]. Additionally, the LLM annotated evidence certainty (sufficient or uncertain) for each question, enabling stratified evaluation and error analysis.

Next, we performed retrieval accessibility checks for each generated question, similar to the round-trip consistency filtering in ARES[60]. Using a system-agnostic hybrid retrieval baseline (combining sparse and dense methods), we retrieved the top- $K$  candidate windows. If the seed window was recalled within top- $K$ , the question was deemed “accessible” and entered the main split; otherwise, it entered the challenge split for manual review.

For reference evidence construction, we selected gold windows for each accessible question from a larger candidate pool. This entailed reranking candidates by relevance, then having the LLM grade the evidence relationship (strongly supportive/supportive/weakly related/unrelated). Strongly supportive and supportive windows formed the gold evidence set. Based on gold windows, we generated hierarchical reference answers: an exact answer summarizing the core conclusion, and an ideal answer organized by evidence grades (A–E), with Grade A prioritized and remaining evidence presented in descending pyramid order. All statements were strictly aligned with gold windows, with source identifiers for traceability. The LLM then decomposed the exact answer into atomic facts (nuggets) for automated assessment[30].

Finally, four sports science graduate students manually reviewed all QA pairs, with particular attention to samples marked “evidence uncertain” and those in the challenge split. Approximately 2,000 questions were generated initially; after human screening, 1,637 were retained as the official evaluation set. We extracted questions, exact answers, and nuggets and compiled them into a public dataset for reusability. Because some gold windows originate from institutionally subscribed materials, the public version excluded evidence window text.

## 4.6 Evaluation Process

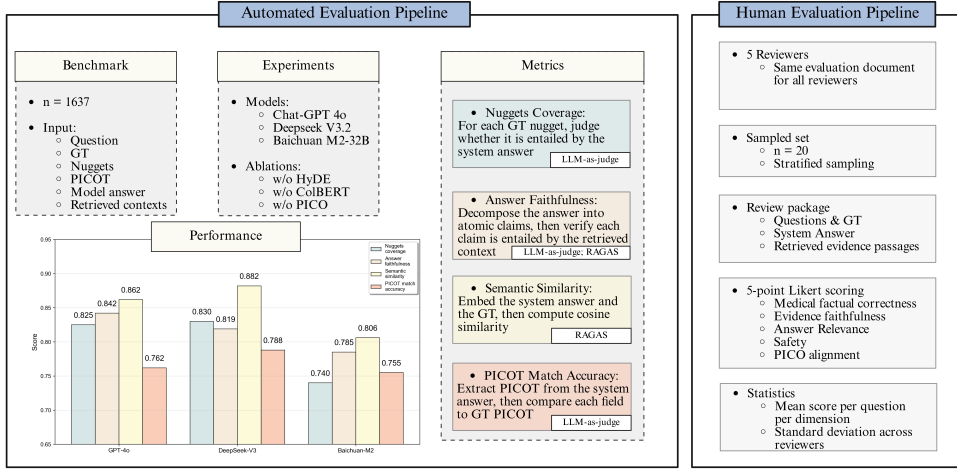


**Fig. 5** Automated and human evaluation pipelines of SR-RAG.

SR-RAG evaluation comprised two dimensions: automated and manual (Fig. 5). For automated evaluation, we used all 1,637 QA pairs to conduct multi-metric assessments across generative models and ablation experiments. Metrics included: (1) Nugget coverage: extent to which the answer covers GT core factual units; (2) Answer faithfulness: whether answer statements are supported by retrieved evidence; (3) Semantic similarity: semantic consistency between answer and GT; (4) PICOT match accuracy: alignment of the answer with P/I/C/O/T elements.

Nugget coverage and PICOT match accuracy were implemented via LLM-as-judge[32]: for each nugget, the LLM determined whether it was covered by the system answer; for each extracted P/I/C/O/T field, the LLM evaluated whether it matched the reference (paraphrasing permitted; missing GT fields default to matched). Coverage and match rates were then aggregated. Answer faithfulness and semantic similarity were assessed via the RAGAS framework[20]. RAGAS first extracted claims from the answer, then determined for each claim whether it was supported by the actually retrieved context, yielding a faithfulness score (also LLM-as-judge based). Semantic similarity was computed as cosine similarity between text embeddings of the system answer and GT.

For manual evaluation, we invited five sports rehabilitation experts to review a random sample of 20 questions, each using identical review materials. Review materials include task instructions, scoring criteria, evaluation dimensions, and the question set. For each question, materials provide the question and GT, system-generated answer, retrieved evidence fragments, and a scoring sheet. A five-point Likert scale was used, with each question scored independently across five dimensions: (1) Medical factual accuracy: whether conclusions, values, and prescriptions align with current evidence, guidelines, and consensus; (2) Answer faithfulness: whether key statements are substantiated by retrieved fragments; (3) Answer relevance: whether the response addresses core concerns and covers key constraints; (4) Safety: whether the answer contains potentially harmful or misleading content; (5) PICOT alignment: whether the answer is structured around the question’s P/I/C/O/T elements without population or intervention mismatch. We aggregated scores from all five experts across five dimensions for the 20 questions and computed means and standard deviations per question and dimension for analysis.

## 4.7 Implementation details

All experiments were implemented in Python 3.11. Graph construction followed YouTU-GraphRAG’s schema-bounded extraction and community compression using NetworkX, with graph artifacts stored as JSON. Dense retrieval was implemented with sentence-transformers and FAISS; candidate lists from dense, graph, and HyDE retrieval were fused via RRF. Two-stage reranking used ColBERT(mxba-edges-colbert-v0) for coarse ranking and a cross-encoder (bge-reranker-v2-m3) for final logits. BETR training used PyTorch 2.6.0 with the Adam optimizer (learning rate: 0.05, epochs: 80,  $K = 20$  negatives per positive). Hyperparameters ( $\tau$ ) were selected via grid search on a query-disjoint split (train:  $n=1,310$ ; validation:  $n=327$ ). Unless otherwise specified, LLM decoding used temperature = 0.

## **Data availability**

The SR-RAG benchmark dataset is publicly available at <https://huggingface.co/datasets/Ning311/sr-rag-benchmark>. The SR-RAG knowledge graph is publicly available at <https://huggingface.co/datasets/Ning311/sr-rag-knowledge-graph>. Because some gold windows originate from institutionally subscribed materials, the public release does not include the full text of evidence windows.

## **Code availability**

The SR-RAG code will be publicly released after publication.

## **Acknowledgements**

We thank the expert clinicians for participating in the human evaluation and providing valuable feedback. This work was supported by the National Key Research and Development Program of China (Grant No. 2022YFC3600201), the National Natural Science Foundation of China (Grant No. 32000838), and the Chinese Universities Scientific Fund (Grant No. 2024JNPD002).

## **Author contributions**

J.Z., J.S., and Y.L. contributed to the conception and design of the study. T.S. and J.Z. designed the BETR algorithm. W.T., Z.L., J.Z., J.S., and Z.W. contributed to data collection and benchmark construction. J.X.L., J.L., and X.L. provided medical expertise and were responsible for the recruitment and execution of the expert clinician evaluation. Y.L. supervised the overall project, reviewed the experimental design and results, and acquired funding. J.Z. and Y.L. drafted and revised the manuscript and approved the final version.

## **Competing interests**

The authors declare no competing interests.

## **Additional information**

This preprint includes supplementary material.

Correspondence and requests for materials should be addressed to the corresponding author.

## Supplementary Materials

### S1. Schema Specifications

Table S1 lists the PICO-extended schema used for graph construction and retrieval. Table S2 lists the PICO-neutral schema used in the *w/o PICO-extended schema* ablation.

**Table S1** PICO-extended schema used in graph construction and retrieval.

Nodes	Relations	Attributes
Population, Condition, Intervention, Comparator, Outcome, Timepoint, Arm, Device, Recommendation, AdverseEvent, Contraindication	has_population, has_condition, uses_intervention, compares_to, reports_outcome, has_timepoint, targets_arm, uses_device, recommends_for, recommends_against, has_adverse_event, contraindicated_for	age_bin, age_range, sex, baseline_severity, time_since_injury_or_surgery, inclusion_criteria, exclusion_criteria, dose, frequency, session_duration, intensity, progression_rule, setting, supervision, followup_weeks, timepoint_value, timepoint_unit, measure_name, outcome_domain, primary_outcome, adverse_event, contraindication, recommendation_strength, evidence_certainty, applicability_notes, study_design, sample_size, protocol_params

**Table S2** PICO-neutral schema used in the *w/o PICO-extended schema* ablation.

Nodes	Relations	Attributes
ClinicalConcept, EvidenceStatement, Study, Guideline, Recommendation, Protocol, OutcomeMeasure, Device, AdverseEvent, Contraindication, Topic	mentions, associated_with, belongs_to_topic, reported_in, supported_by, has_protocol, uses_device, reports_measure, recommends_for, recommends_against, has_adverse_event, contraindicated_for	age_bin, age_range, sex, baseline_severity, time_since_injury_or_surgery, inclusion_criteria, exclusion_criteria, dose, frequency, session_duration, intensity, progression_rule, setting, supervision, followup_weeks, timepoint_value, timepoint_unit, measure_name, outcome_domain, primary_outcome, adverse_event, contraindication, recommendation_strength, evidence_certainty, applicability_notes, study_design, sample_size, protocol_params

## S2. Prompt Templates

This section provides representative prompt excerpts used in SR-RAG. For brevity, we include only the core instructions and output constraints.

### *PICO-guided HyDE.*

#### **Listing S1** PICO-guided HyDE prompt excerpt.

```
You are a sports rehabilitation clinician.  
Write a concise, evidence-style passage that answers the question, explicitly following PICOT:  
- P: population characteristics and key constraints  
- I: intervention details (dose/frequency/intensity/progression)  
- C: comparator if applicable  
- O: outcomes and relevant measures  
- T: time horizon / follow-up  
  
Constraints:  
- Do NOT cite sources.  
- Use neutral clinical language.  
- 5-8 sentences, concise, declarative, paper-like.  
  
Question:  
{question}  
  
Output ONLY the hypothetical evidence window.
```

In practice, we invoke this template multiple times per query to obtain diversified hypothetical windows.

### *Evidence window selection.*

#### **Listing S2** Evidence window selection prompt excerpt.

```
You are an evidence extraction assistant. Given a question and a medical passage,  
identify up to MAX contiguous snippets from the passage that directly help answer the question.  
Each snippet must be copied verbatim and kept short.  
Return strictly JSON:  
{  
  "windows": [  
    {  
      "snippet": "...",  
      "reason": "...",  
      "contains_population": true/false,  
      "contains_intervention": true/false,  
      "contains_comparator": true/false,  
      "contains_outcome": true/false,  
      "contains_time": true/false,  
      "outcome_and_time_same_window": true/false  
    }  
  ]  
}  
Question: {question}  
Passage: <<<{passage}>>>
```

### *Nugget coverage.*

#### **Listing S3** Nugget coverage prompt excerpt.

```
You are a clinical QA evaluator.  
Given the question, a system answer, and ONE ground-truth nugget,  
judge whether the nugget is explicitly covered by the system answer.
```

```

Rules:
- Only judge coverage by the system answer text itself.
- Treat synonymous expressions as covered.
- If the nugget is contradicted or missing, mark it as not covered.
- Output RFC8259-compliant JSON only.

Return JSON:
{
  "covered": true/false,
  "reason": "brief justification"
}

Question: {question}
System answer: {answer}
GT nugget: {nugget}

```

### ***PICOT match accuracy.***

#### ***Listing S4*** PICOT match prompt excerpt.

```

You are a medical information extraction and matching assistant.
Given gold PICOT fields and the system answer, extract PICOT from the system answer and compare
field-by-field.

Rules:
- Do not invent missing fields. If a field is not stated, output null.
- Consider medically equivalent synonyms as a match.
- Exclude GT fields that are explicitly marked as null/missing from scoring.
- Output RFC8259-compliant JSON only.

Return JSON:
{
  "system_picot": {"P": "...|null", "I": "...|null", "C": "...|null", "O": "...|null", "T": "...|null"},
  "match": {"P": 0/1, "I": 0/1, "C": 0/1, "O": 0/1, "T": 0/1},
  "reason": {"P": "...", "I": "...", "C": "...", "O": "...", "T": "..."}
}

Question: {question}
Gold PICOT: {gold_picot}
System answer: {answer}

```

## **S3. Key Hyperparameters and BETR Training Details**

Table [S3](#) summarizes selected hyperparameters for SR-RAG and BETR. Evidence grades were defined as: A = guidelines/expert consensus; B = systematic reviews/meta-analyses; C = randomized controlled trials; D = cohort studies; E = other studies.

## **S4. Benchmark Composition by Sub-condition**

Table [S4](#) summarizes the SR-RAG benchmark composition (n = 1,637 queries). The benchmark covers 21 common sports rehabilitation sub-conditions, along with two cross-condition guideline sets. Specifically, the guideline sets include a general guideline set and a special-population subset.

**Table S3** Selected hyperparameters and training settings.

Item	Setting
<b>SR-RAG retrieval and reranking</b>	
Final evidence budget	Top- $K$ contexts = 12; soft quota: retain $\geq 1$ Grade A if its score is sufficiently high
Recall capacities	dense top- $K$ = 300; graph top- $K$ = 120; HyDE passages retrieved via dense top- $K$ = 300; RRF $k$ = 60
HyDE	3 hypothetical passages per query; temperature = 0.3 for lexical diversification
Window selection	window size = 320 tokens; max windows/chunk = 3; overlap = 64 tokens
Two-stage reranking	ColBERT $\rightarrow$ cross-encoder
<b>BETR</b>	
Data split	query-disjoint train/validation: 1310/327 queries; 21,546/5,209 pairs
Pair construction	20 negatives per positive
Optimization	Adam, learning rate 0.05, epochs 80, seed 42
Shrinkage strength	$\tau$ selected via grid search on validation; selected $\tau$ = 1.0 and fixed for all experiments
Scale prior	$\sigma_a = 5.0$ ; reparameterized $a = \exp\{\alpha\}$
Learned parameters	$a = 1.0348$ ; $u_A = 0$ , $u_B = -0.1287$ , $u_C = -0.2575$ , $u_D = -0.3863$ , $u_E = -0.5151$

**Table S4** SR-RAG benchmark composition by sub-condition and guideline set.

Code	Sub-condition / Guideline set	Queries (n)
<b>Guideline sets</b>		
GL-GEN	General clinical exercise guideline set	92
GL-SP	Special-population guideline subset	11
<b>Sub-conditions</b>		
ACL	Anterior cruciate ligament injury	46
AT	Achilles tendinopathy	36
BSI	Bone stress injury	38
FS	Adhesive capsulitis of the shoulder	79
GPA	Groin pain in athletes	79
GTPS	Greater trochanteric pain syndrome	96
HSI	Hamstring strain injury	70
IS	Isthmic spondylolisthesis	105
LAS	Lateral ankle sprain	86
LBP	Low back pain	50
ITBS	Iliotibial band syndrome	98
LET	Lateral elbow tendinopathy	70
MACL	Knee meniscal and articular cartilage lesions	78
MTSS	Medial tibial stress syndrome	55
NAHJP	Nonarthritic hip joint pain	73
NP	Neck pain	63
PHP	Plantar heel pain	76
PFP	Patellofemoral pain	87
PT	Patellar tendinopathy	77
RCRSP	Rotator cuff related shoulder pain	102
FTASD	First-time anterior shoulder dislocation	70

## References

- [1] Barba, N., Shin, J. Y., Hiremath, G. & Lauff, C. A. Exploring health educational interventions for children with congenital heart disease: Scoping review. *JMIR Pediatrics and Parenting* **8**, e64814 (2025). URL <https://pediatrics.jmir.org/2025/1/e64814>.
- [2] Ubeda Tikkanen, A. *et al.* Core components of a rehabilitation program in pediatric cardiac disease. *Frontiers in Pediatrics* **11** (2023). URL <https://www.frontiersin.org/journals/pediatrics/articles/10.3389/fped.2023.1104794/full>. Publisher: Frontiers.
- [3] Interamerican Society of Cardiology (SIAC). 2024 SIAC guidelines on cardiorespiratory rehabilitation in pediatric patients with congenital heart disease. *Revista Española de Cardiología (English Edition)* **77**, 680–689 (2024). URL <https://www.revespcardiol.org/en-2024-siac-guidelines-on-cardiorespiratory-articulo-S1885585724001543>. Publisher: Elsevier.
- [4] Hager, P. *et al.* Evaluation and mitigation of the limitations of large language models in clinical decision-making. *Nature Medicine* **30**, 2613–2622 (2024). URL <https://www.nature.com/articles/s41591-024-03097-1>. Publisher: Nature Publishing Group.
- [5] American College of Sports Medicine. *ACSM's Guidelines for Exercise Testing and Prescription* 12th edn (Wolters Kluwer, 2025). URL <https://shop.lww.com/ACSM-s-Guidelines-for-Exercise-Testing-and-Prescription/p/9781975219215>.
- [6] Almaadawy, O. *et al.* Target Heart Rate Formulas for Exercise Stress Testing: What Is the Evidence? *Journal of Clinical Medicine* **13** (2024). URL <https://www.mdpi.com/2077-0383/13/18/5562>. Company: Multidisciplinary Digital Publishing Institute Distributor: Multidisciplinary Digital Publishing Institute Institution: Multidisciplinary Digital Publishing Institute Label: Multidisciplinary Digital Publishing Institute Publisher: publisher.
- [7] Lauer, M. S. *et al.* Impaired Chronotropic Response to Exercise Stress Testing as a Predictor of Mortality. *JAMA* **281**, 524–529 (1999). URL <https://doi.org/10.1001/jama.281.6.524>.
- [8] Lewis, P. *et al.* Retrieval-Augmented Generation for Knowledge-Intensive NLP Tasks. *Advances in Neural Information Processing Systems* **33**, 9459–9474 (2020). URL <https://proceedings.neurips.cc/paper/2020/hash/6b493230205f780e1bc26945df7481e5-Abstract.html>.
- [9] Yang, R. *et al.* Retrieval-augmented generation for generative artificial intelligence in health care. *npj Health Systems* **2**, 2 (2025). URL <https://www.nature.com/articles/s44401-024-00004-1>.

- [10] Béchard, P. & Ayala, O. M. Reducing hallucination in structured outputs via Retrieval-Augmented Generation. *Proceedings of the 2024 Conference of the North American Chapter of the Association for Computational Linguistics: Human Language Technologies (Volume 6: Industry Track)* 228–238 (2024). URL <http://arxiv.org/abs/2404.08189>.
- [11] Luan, Y., Eisenstein, J., Toutanova, K. & Collins, M. Sparse, Dense, and Attentional Representations for Text Retrieval. *Transactions of the Association for Computational Linguistics* **9**, 329–345 (2021). URL <https://aclanthology.org/2021.tacl-1.20/>.
- [12] Shi, Y. *et al.* MKRAG: Medical Knowledge Retrieval Augmented Generation for Medical Question Answering. *AMIA Annual Symposium Proceedings* (2024). URL <https://arxiv.org/abs/2309.16035>.
- [13] Sohn, J., Jeong, M., Sung, M. & Kang, J. RAG<sup>2</sup>: Rationale-Guided Retrieval Augmented Generation for Medical Question Answering. *Proceedings of the 2025 Conference of the North American Chapter of the Association for Computational Linguistics* 635–650 (2025). URL <https://aclanthology.org/2025.naacl-long.635>.
- [14] Sun, W., Chen, J. *et al.* MRD-RAG: Enhancing Medical Diagnosis with Multi-Round Retrieval-Augmented Generation. *arXiv preprint arXiv:2504.07724* (2025). URL <https://arxiv.org/abs/2504.07724>.
- [15] Gupta, S., Ranjan, R. & Singh, S. N. A comprehensive survey of retrieval-augmented generation (RAG): Evolution, current landscape and future directions. *arXiv preprint arXiv:2410.12837* (2024). URL <https://arxiv.org/abs/2410.12837>.
- [16] Xiong, G., Jin, Q., Lu, Z. & Zhang, A. Benchmarking retrieval-augmented generation for medicine. *Findings of the Association for Computational Linguistics: ACL 2024* 6233–6251 (2024). URL <https://aclanthology.org/2024.findings-acl.372/>.
- [17] Asai, A., Wu, Z., Wang, Y., Sil, A. & Hajishirzi, H. Self-RAG: Learning to retrieve, generate, and critique through self-reflection. *Proceedings of the Twelfth International Conference on Learning Representations (ICLR)* (2024). URL <https://arxiv.org/abs/2310.11511>.
- [18] Yan, S.-Q., Gu, J.-C., Zhu, Y. & Ling, Z.-H. Corrective retrieval augmented generation. *arXiv preprint arXiv:2401.15884* (2024). URL <https://arxiv.org/abs/2401.15884>.
- [19] Huang, L. *et al.* A survey on hallucination in large language models: Principles, taxonomy, challenges, and open questions. *ACM Transactions on Information Systems* **43**, 1–55 (2024). URL <https://dl.acm.org/doi/10.1145/3703155>.

- [20] Es, S., James, J., Espinosa Anke, L. & Schockaert, S. RAGAs: Automated Evaluation of Retrieval Augmented Generation. *Proceedings of the 18th Conference of the European Chapter of the Association for Computational Linguistics: System Demonstrations* 150–158 (2024). URL <https://aclanthology.org/2024.eacl-demo.16/>.
- [21] Sun, M., Zhao, S., Chen, J., Wang, H. & Qin, B. META-RAG: Meta-analysis-inspired evidence-re-ranking method for retrieval-augmented generation in evidence-based medicine. *arXiv preprint arXiv:2510.24003* (2025). URL <https://arxiv.org/abs/2510.24003>.
- [22] Guyatt, G. H. *et al.* GRADE: an emerging consensus on rating quality of evidence and strength of recommendations. *BMJ* **336**, 924–926 (2008). URL <https://www.bmj.com/content/336/7650/924>.
- [23] Sackett, D. L., Rosenberg, W. M. C., Gray, J. A. M., Haynes, R. B. & Richardson, W. S. Evidence based medicine: what it is and what it isn't. *BMJ* **312**, 71–72 (1996). URL <https://www.bmj.com/content/312/7023/71>.
- [24] Edge, D. *et al.* From local to global: A graph RAG approach to query-focused summarization. *arXiv preprint arXiv:2404.16130* (2024). URL <https://arxiv.org/abs/2404.16130>.
- [25] Cabello, L., Suster, S. & Hershcovich, D. MEG: Medical knowledge-augmented large language models for question answering. *arXiv preprint arXiv:2411.03883* (2024). URL <https://arxiv.org/abs/2411.03883>.
- [26] Dong, Y. *et al.* Youtu-GraphRAG: Vertically unified agents for graph retrieval-augmented complex reasoning. *arXiv preprint arXiv:2508.19855* (2025). URL <https://arxiv.org/abs/2508.19855>.
- [27] Gao, L., Ma, X., Lin, J. & Callan, J. Precise zero-shot dense retrieval without relevance labels. *Proceedings of the 61st Annual Meeting of the Association for Computational Linguistics (Volume 1: Long Papers)* 1762–1777 (2023).
- [28] Cormack, G. V., Clarke, C. L. A. & Büttcher, S. Reciprocal rank fusion outperforms condorcet and individual rank learning methods. *Proceedings of the 32nd International ACM SIGIR Conference on Research and Development in Information Retrieval* 758–759 (2009).
- [29] Khattab, O. & Zaharia, M. ColBERT: Efficient and effective passage search via contextualized late interaction over BERT. *Proceedings of the 43rd International ACM SIGIR Conference on Research and Development in Information Retrieval* 39–48 (2020).
- [30] Min, S. *et al.* FActScore: Fine-grained atomic evaluation of factual precision in long form text generation. *Proceedings of the 2023 Conference on Empirical*

*Methods in Natural Language Processing* 12076–12100 (2023).

- [31] Lin, J., Pradeep, R., Sethi, S. & Wang, S. Initial nugget evaluation results for the TREC 2024 RAG track with the AutoNuggetizer framework. *arXiv preprint arXiv:2411.09607* (2024). URL <https://arxiv.org/abs/2411.09607>.
- [32] Zheng, L. *et al.* Judging LLM-as-a-judge with MT-Bench and chatbot arena. *Advances in Neural Information Processing Systems* **36** (2023). URL <https://arxiv.org/abs/2306.05685>.
- [33] OpenAI. GPT-4o system card. *arXiv preprint arXiv:2410.21276* (2024). URL <https://arxiv.org/abs/2410.21276>.
- [34] Baichuan AI. Baichuan-M2: Scaling medical capability with large verifier system. *arXiv preprint arXiv:2509.02208* (2025). URL <https://arxiv.org/abs/2509.02208>.
- [35] DeepSeek-AI. DeepSeek-V3 technical report. *arXiv preprint arXiv:2412.19437* (2024). URL <https://arxiv.org/abs/2412.19437>.
- [36] Newman-Griffis, D. *et al.* Ambiguity in medical concept normalization: An analysis of clinical concept overlap in health records. *Journal of the American Medical Informatics Association* **28**, 516–524 (2021).
- [37] Sun, M., Zhao, S., Wang, H. & Qin, B. PICOs-RAG: PICO-supported query rewriting for retrieval-augmented generation in evidence-based medicine. *arXiv preprint arXiv:2510.23998* (2025). URL <https://arxiv.org/abs/2510.23998>.
- [38] Wang, L., Yang, N. & Wei, F. Query2doc: Query expansion with large language models. *Proceedings of the 2023 Conference on Empirical Methods in Natural Language Processing* 9414–9423 (2023).
- [39] Zhu, W., Zhao, L., Yu, C., Huang, S. & Liu, Z. HyQE: Ranking contexts with hypothetical query embeddings. *Findings of the Association for Computational Linguistics: EMNLP 2024* 13024–13036 (2024).
- [40] Wang, X. *et al.* Large language models driving evidence-based clinical decision making. *npj Digital Medicine* (2025).
- [41] Wang, S. *et al.* Med-R<sup>2</sup>: Crafting trustworthy LLM physicians via retrieval and reasoning of evidence-based medicine. *arXiv preprint arXiv:2501.11885* (2025). URL <https://arxiv.org/abs/2501.11885>.
- [42] Li, W. *et al.* Refine medical diagnosis using generation augmented retrieval and clinical practice guidelines. *arXiv preprint arXiv:2506.21615* (2025). URL <https://arxiv.org/abs/2506.21615>.
- [43] Xia, H. *et al.* Language and multimodal models in sports: A survey of datasets and applications. *arXiv preprint arXiv:2406.12252* (2024). URL <https://arxiv.org/abs/2406.12252>.

- org/abs/2406.12252.
- [44] Musat, C.-L. *et al.* Diagnostic applications of AI in sports: A comprehensive review of injury risk prediction methods. *Diagnostics* **14**, 2516 (2024).
- [45] Reis, F. J. J., Alaiti, R. K., Vallio, C. S. & Hespanhol, L. Artificial intelligence and machine learning approaches in sports: Concepts, applications, challenges, and future perspectives. *Brazilian Journal of Physical Therapy* **28**, 101083 (2024).
- [46] OCEBM Levels of Evidence Working Group. The Oxford Levels of Evidence 2 (2011). URL <https://www.cebm.ox.ac.uk/resources/levels-of-evidence/ocebm-levels-of-evidence>. Oxford Centre for Evidence-Based Medicine.
- [47] National Health and Medical Research Council. NHMRC additional levels of evidence and grades for recommendations for developers of guidelines. Tech. Rep., Australian Government (2009). URL <https://www.nhmrc.gov.au>.
- [48] Joanna Briggs Institute. JBI levels of evidence (2014). URL [https://jbi.global/sites/default/files/2019-05/JBI-Levels-of-evidence\\_2014\\_0.pdf](https://jbi.global/sites/default/files/2019-05/JBI-Levels-of-evidence_2014_0.pdf).
- [49] Auer, C. *et al.* Docling technical report. *arXiv preprint arXiv:2408.09869* (2024). URL <https://arxiv.org/abs/2408.09869>.
- [50] Chase, H. LangChain (2022). URL <https://github.com/langchain-ai/langchain>.
- [51] Jain, A., Aggarwal, P. & Saladi, A. AutoChunker: Structured text chunking and its evaluation. *Proceedings of the 63rd Annual Meeting of the Association for Computational Linguistics (Volume 6: Industry Track)* 983–995 (2025).
- [52] Zhao, J. *et al.* Meta-chunking: Learning text segmentation and semantic completion via logical perception. *arXiv preprint arXiv:2410.12788* (2024). URL <https://arxiv.org/abs/2410.12788>.
- [53] Duarte, A. V. *et al.* LumberChunker: Long-form narrative document segmentation. *Findings of the Association for Computational Linguistics: EMNLP 2024* (2024). URL <https://arxiv.org/abs/2406.17526>.
- [54] Burges, C. *et al.* Learning to rank using gradient descent. *Proceedings of the 22nd International Conference on Machine Learning* 89–96 (2005).
- [55] Bradley, R. A. & Terry, M. E. Rank analysis of incomplete block designs: I. the method of paired comparisons. *Biometrika* **39**, 324–345 (1952).
- [56] Gelman, A. *et al.* *Bayesian Data Analysis* 3rd edn (Chapman and Hall/CRC, 2013).
- [57] Takehi, R., Clavié, B., Lee, S. & Shakir, A. Fantastic (small) retrievers and how to train them: mxbai-edge-colbert-v0 tech report. *arXiv preprint arXiv:2510.14880*

- (2025). URL <https://arxiv.org/abs/2510.14880>.
- [58] Martínez Rivera, E. & Menolascina, F. ModernBERT + ColBERT: Enhancing biomedical RAG through an advanced re-ranking retriever. *arXiv preprint arXiv:2510.04757* (2025). URL <https://arxiv.org/abs/2510.04757>.
  - [59] Chen, J. *et al.* BGE M3-embedding: Multi-lingual, multi-functionality, multi-granularity text embeddings through self-knowledge distillation. *arXiv preprint arXiv:2402.03216* (2024). URL <https://arxiv.org/abs/2402.03216>.
  - [60] Saad-Falcon, J., Khattab, O., Potts, C. & Zaharia, M. ARES: An automated evaluation framework for retrieval-augmented generation systems. *Proceedings of the 2024 Conference of the North American Chapter of the Association for Computational Linguistics: Human Language Technologies* 338–354 (2024).